A Local Model of Light Interaction with Transparent Crystalline Media

Victor A. Debelov and Dmitry S. Kozlov

Abstract—The paper is devoted to the derivation of a bidirectional distribution function for crystals, which specifies all outgoing rays for a ray coming to the boundary of two transparent crystalline media with different optical properties, i.e., a particular mineral, directions of optical axes if they exist, and other features. A local model of interaction based on the notion of polarized light ray is introduced, which is specified by a geometric ray, its polarization state, light intensity, and so on. The computational algorithm that is suggested allows computing the directions and other properties of all (up to four) outgoing rays. In this paper, isotropic, uniaxial, and biaxial crystals are processed in a similar manner. The correctness of the model is validated by comparison of photos of real uniaxial crystals with corresponding computed images. The case of biaxial crystals is validated by testing the effect of conical refraction. Specifications of a series of tests devoted to rendering of optically different objects is presented also.

Index Terms—Isotropic crystal, uniaxial crystal, biaxial crystal, crystalline aggregate, optical axis, polarized ray, optical dispersion, birefringence, conical refraction, photorealistic rendering, ray tracing

1 Introduction

The rendering of anisotropic transparent and translucent crystals is a specific area of computer graphics, so not many papers are devoted to this problem. In many papers, the importance of gemstone rendering was shown. If a physically correct renderer of crystals is available, it could be used in other practical areas, especially in education, e.g., in simulation of complex devices like petrographic microscope.

All translucent crystals (and media) can be divided into isotropic, uniaxial, and biaxial ones depending on the number of optical axes: 0 (isotropic crystals), 1 (uniaxial crystals), or 2 (biaxial crystals), respectively. In natural conditions, the crystals can be affected by various forces (pressure, electromagnetic fields, etc.), and a real uniaxial crystal can behave as an optically biaxial one. For instance, in certain conditions, vacuum (e.g., Kerr effect) behaves as an anisotropic medium with respect to light, that is, it demonstrates birefringence. In practice, these changes are insignificant and may not be taken into account. In this paper, we deal with ideal crystals.

A central problem is a determination of a light ray path through a boundary between two different media. The books on crystal optics usually do not care about applications of computer graphics and, therefore, do not contain the required formulas, which have to be developed specially. Papers [1] and [2] consider interactions of a light ray with a boundary between an isotropic and uniaxial media. Paper [3] describes an uniform algorithm to calculate interaction of a light ray with a boundary between isotropic and uniaxial media and a boundary between two different uniaxial media, e.g., a boundary between two single forms of the same crystalline aggregate. Paper [4] deals with a boundary between an isotropic medium and a uniaxial or biaxial crystal. The algorithm is limited to calculation of refracted rays only. Calculation of reflected rays and energy relations that are necessary to compute photorealistic images are absent. The work [5] is devoted to the case of a boundary between isotropic and biaxial media. We should note that authors have derived similar final computational formulas as presented in this paper for the analogous boundary.

Remark. A derivation of final formulas is very important as it determines parts of algorithms devoted to computation of particular parameters of a final formula. To derive a final formula, a trigonometric approach is often used as in [2], [4], and [5], although there are also papers in which matrix calculations are employed, e.g., the paper [6]. Our derivation for construction of rays is based on a covariant method [7], which is independent of the coordinate system and allows us to construct closed-form formulas and an uniform algorithm for calculating of the interaction of a ray with the interface between isotropic, uniaxial, and biaxial media.

Algorithms presented in works [1], [2], and [3] are based on closed-form formulas while ones in [4], [5] include numerical calculations of certain parameters.

All mentioned papers deal with a boundary between isotropic and anisotropic media. For the first time, we present algorithm that processes uniformly interactions between light rays and a boundary between two media of

- *V.A. Debelov is with the Laboratory of Numerical Analysis and Computer Graphics, Institute of Computational Mathematics and Mathematical Geophysics, Siberian Branch of Russian Academy of Sciences, prospect Akademika Lavrentjeva, 6, Novosibirsk 630090, Russia. E-mail: debelov@oapmg.sscc.ru.*
- *D.S. Kozlov is with the Laboratory of Numerical Analysis and Computer Graphics, Institute of Computational Mathematics and Mathematical Geophysics, Siberian Branch of Russian Academy of Sciences, prospect Akademika Lavrentjeva, 6, Novosibirsk 630090, Russia, and Novosibirsk State University. E-mail: kozlov@oapmg.sscc.ru.*

Manuscript received 30 Dec. 2011; revised 17 July 2012; accepted 20 Oct. 2012; published online 26 Oct. 2012.
Recommended for acceptance by K. Bala.
For information on obtaining reprints of this article, please send e-mail to: tvcg@computer.org, and reference IEEECS Log Number TVCG-2011-12-0323.
Digital Object Identifier no. 10.1109/TVCG.2012.304.

arbitrary optical types. It is an extension of the paper [3] to the biaxial case.

In this paper, analogously to other works, only plane electromagnetic waves [7], [8], that is, classical solutions to Maxwells equations, are considered. In Sections 2 and 3, notation used is presented. Section 4 is devoted to formulas of ray propagation in transparent media. Section 5 deals with the interaction of a ray with the boundary between two media. In Section 6, the representation of light polarization being used is considered. In what follows, the following concepts will be used: ray, state of ray polarization, coherence matrix, and so on. Whereas in some papers Jones vectors or Müller matrices are used to describe the state of light polarization [2], we use coherence matrices and their modifiers, as in [9]. Thus, Sections 2, 3, 4, 5, and 6 describe necessary information from optics. Although we focus on known facts from physical optics, an analogous derivation is absent in a literature. The most of presented equations are used while calculation of parameters of a final formula. In Section 7, our contribution, a detailed stepwise description of an algorithm to calculate the interaction of a ray with the boundary between two media is presented. Numerical experiments are described in Section 8. In the end, a reader can find list of important symbols used in the paper.

2 Notation

In this paper, we apply unusual to graphics audience notation for dot and vector products, and so on. We follow the style of the book [7].

A column vector $\mathbf{u} = (u_1 u_2 u_3)^T$.

A second-rank tensor is a 3×3 matrix

$$\alpha = \begin{pmatrix} \alpha_{11} & \alpha_{12} & \alpha_{13} \\ \alpha_{21} & \alpha_{22} & \alpha_{23} \\ \alpha_{31} & \alpha_{32} & \alpha_{33} \end{pmatrix}.$$

If some quantities (tensors or vectors) are placed alongside each other without any sign between them, this implies their convolution, that is, summation over neighboring indices. For instance, $\mathbf{uv}$ is the scalar product of two vectors

$$\mathbf{uv} = u_1 v_1 + u_2 v_2 + u_3 v_3.$$

Convolution of a matrix with a vector is defined as the product of the matrix and the vector as follows:

$$\alpha \mathbf{u} = \begin{pmatrix} \alpha_{11} u_1 + \alpha_{12} u_2 + \alpha_{13} u_3 \\ \alpha_{21} u_1 + \alpha_{22} u_2 + \alpha_{23} u_3 \\ \alpha_{31} u_1 + \alpha_{32} u_2 + \alpha_{33} u_3 \end{pmatrix}.$$

It should be noted that the quantity $\mathbf{u}\alpha\mathbf{v}$ is a scalar.

The following classical vector product is defined for any two vectors:

$$[\mathbf{uv}] = \mathbf{u} \times \mathbf{v} = \begin{pmatrix} 0 & -u_3 & u_2 \\ u_3 & 0 & -u_1 \\ -u_2 & u_1 & 0 \end{pmatrix} \mathbf{v} = \mathbf{u}^{\times} \mathbf{v},$$

and the tensor $\mathbf{u}^{\times}$ is called the dual one to the vector $\mathbf{u}$.

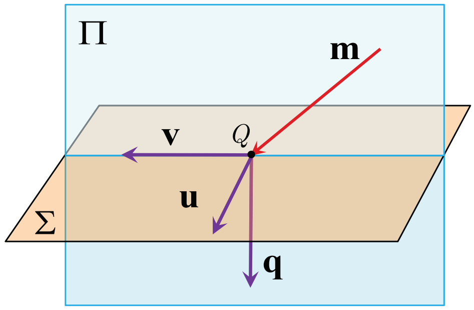

Fig. 1. Local system of coordinates and notations.

The special tensor

$$\mathbf{u} \cdot \mathbf{v} = \begin{pmatrix} u_1 v_1 & u_1 v_2 & u_1 v_3 \\ u_2 v_1 & u_2 v_2 & u_2 v_3 \\ u_3 v_1 & u_3 v_2 & u_3 v_3 \end{pmatrix}$$

is called the dyad of two vectors.

A scalar k is equivalent to the following diagonal matrix:

$$k = diag(k, k, k).$$

The matrix

$$\bar{\alpha} = \begin{pmatrix} A_{11} & A_{21} & A_{31} \\ A_{12} & A_{22} & A_{32} \\ A_{13} & A_{23} & A_{33} \end{pmatrix}$$

is the adjoint matrix of α; here, A_{ij} is the (i, j) cofactor of α. If determinant $|\alpha| \neq 0$, the inverse matrix $\alpha^{-1} = \frac{1}{|\alpha|}\bar{\alpha}$.

The trace of a matrix α is the sum $\alpha_t = \alpha_{11} + \alpha_{22} + \alpha_{33}$.

3 Local Coordinate System

In Fig. 1, we consider a ray falling onto a boundary between media at the point Q. The vector $\mathbf{m}$ is the phase propagation vector, i.e., the normal to the wave surface. The medium from which the ray comes will be called the *first* one. Each medium is characterized by its type: isotropic, uniaxial, or biaxial. A uniaxial crystal has an optical axis $\mathbf{c}$, a biaxial medium has two optical axes $\mathbf{c}_1, \mathbf{c}_2$ (binormals). It is assumed that the optical axes are *unit* vectors.

Consider a Cartesian system of coordinates with origin at point Q. We introduce the following notation:

1. $\mathbf{q}$—unit normal to the boundary directed into the *second* medium.
2. Σ—tangent plane at point Q.
3. Π—plane of incidence formed by vectors $\mathbf{q}$ and $\mathbf{m}$.
4. $\mathbf{u} = \frac{[\mathbf{mq}]}{|[\mathbf{mq}]|}$—unit normal to the plane Π.
5. $\mathbf{v} = [\mathbf{qu}]$.

In the system of coordinates $\mathbf{q}$, $\mathbf{u}$, and $\mathbf{v}$ form a basis.

4 Peculiarities of Ray Propagation in Anisotropic Media

Most transparent media are anisotropic. In such media, classical laws of light reflection and refraction (like Snell's law) are not valid, because in this case, birefringence and *double reflection* can be observed.

An electromagnetic field in any medium is determined by vectors of electric $\mathbf{E}$ and magnetic $\mathbf{H}$ fields and by the vectors of electric induction $\mathbf{D}$ and magnetic induction $\mathbf{B}$. These vectors are described in space and time by Maxwell's equations, which are presented in the following way in the absence of currents and free charges [7], [8]:

$$rot\mathbf{H} = \frac{1}{c}\frac{\partial \mathbf{D}}{\partial t}, rot\mathbf{E} = -\frac{1}{c}\frac{\partial \mathbf{B}}{\partial t}, div\mathbf{D} = 0, div\mathbf{B} = 0. \quad (1)$$

The vectors $\mathbf{E}, \mathbf{D}$ and $\mathbf{H}, \mathbf{B}$ are related by the material equations describing electromagnetic properties of the medium:

$$\mathbf{D} = \varepsilon\mathbf{E}, \mathbf{B} = \mu\mathbf{H}. \quad (2)$$

Here, ε is the permittivity tensor of the medium, and μ is the magnetic tensor. Since only nonmagnetic media are considered, $\mu = 1$ and the vector of magnetic induction $\mathbf{B}$ is identical to the vector $\mathbf{H}$.

Consider solutions to Maxwell's equations in the form of harmonic plane waves. The vectors $\mathbf{E}$ and $\mathbf{H}$ presented in time and space are as follows:

$$\mathbf{E} = \mathbf{E}_0 e^{i\phi}, \mathbf{H} = \mathbf{H}_0 e^{i\phi}, \quad (3)$$

where $\phi = \omega(t - \frac{1}{c}\mathbf{mr})$. The quantities $\mathbf{E}_0$ and $\mathbf{H}_0$ are complex vector amplitudes of electric and magnetic fields, respectively, c is the light speed in vacuum, ω is the circular frequency, $\mathbf{m} = n\mathbf{n}$ is the phase propagation vector (the direction of wave front propagation), n is the phase refractive index (phase propagation speed to light speed in vacuum ratio), $\mathbf{n}$ is the unit vector of phase normal, and $\mathbf{r}$ is the radius vector in a Cartesian system of coordinates. To describe the interaction of harmonic plane waves with nonmagnetic media ($\mu = 1$), the system of (1), (2) can be reduced to the following form [7]:

$$\mathbf{D} = -[\mathbf{mH}], \mathbf{H} = [\mathbf{mE}], \mathbf{D} = \varepsilon\mathbf{E}, \mathbf{B} = \mathbf{H}. \quad (4)$$

It follows from the law of energy conservation that the permittivity tensor 3×3 must be symmetric (see, for instance, [8]), that is, only six of the nine coefficients are independent; here $\varepsilon_{ij} = \varepsilon_{ji}$:

$$\varepsilon = \begin{pmatrix} \varepsilon_{11} & \varepsilon_{12} & \varepsilon_{13} \\ \varepsilon_{21} & \varepsilon_{22} & \varepsilon_{23} \\ \varepsilon_{31} & \varepsilon_{32} & \varepsilon_{33} \end{pmatrix}. \quad (5)$$

The form of the permittivity tensor depends on the system of coordinates in which it is specified. In the principal system of coordinates of the tensor $\{\mathbf{a}_1, \mathbf{a}_2, \mathbf{a}_3\}$, it is represented by a diagonal matrix. The values in the main diagonal are principal permittivities. For an isotropic medium,

$$\varepsilon = diag(\varepsilon_i, \varepsilon_i, \varepsilon_i). \quad (6)$$

As a result, the vectors $\mathbf{D}$ and $\mathbf{E}$ are collinear. For a uniaxial medium, only two of the three coefficients are the same:

$$\varepsilon = diag(\varepsilon_o, \varepsilon_o, \varepsilon_e). \quad (7)$$

For a biaxial medium, all three values differ

$$\varepsilon = diag(\varepsilon_1, \varepsilon_2, \varepsilon_3), \quad (8)$$

indices should be selected so that $\varepsilon_1 < \varepsilon_2 < \varepsilon_3$.

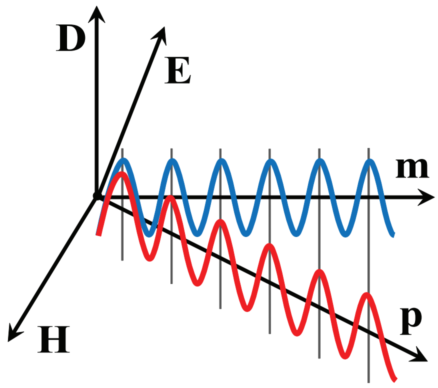

Fig. 2. Structure of an electromagnetic wave in anisotropic media. Note the difference between the directions of energy $\mathbf{p}$ and phase propagation $\mathbf{m}$ in an anisotropic medium.

Introduce the following notation: n_i is the refractive index for an isotropic medium, n_o and n_e are the main refractive indices for a uniaxial medium, and n_1, n_2, n_3 the main refractive indices for a biaxial medium. It is well known that

$$\varepsilon = n^2, \varepsilon_o = n_o^2, \varepsilon_e = n_e^2, \varepsilon_1 = n_1^2, \varepsilon_2 = n_2^2, \varepsilon_3 = n_3^2. \quad (9)$$

For uniaxial media, the optical axis is determined as $\mathbf{c} = \mathbf{a}_3$. For biaxial media, the optical axes (binormals) can be calculated as $\mathbf{c}_1 = k_1\mathbf{a}_1 + k_3\mathbf{a}_3$, $\mathbf{c}_2 = k_1\mathbf{a}_1 - k_3\mathbf{a}_3$, where

$$k_1 = \sqrt{\frac{\varepsilon_3(\varepsilon_2 - \varepsilon_1)}{\varepsilon_2(\varepsilon_3 - \varepsilon_1)}}, k_3 = \sqrt{\frac{\varepsilon_1(\varepsilon_3 - \varepsilon_2)}{\varepsilon_2(\varepsilon_3 - \varepsilon_1)}}.$$

The permittivity tensor of a biaxial medium can be calculated on the base of directions of optical axes (binormals) [7]:

$$\varepsilon = \left(\frac{1}{\varepsilon_2} + \frac{1}{2}\left(\frac{1}{\varepsilon_1} - \frac{1}{\varepsilon_3}\right)(\mathbf{c}_1 \cdot \mathbf{c}_2 + \mathbf{c}_2 \cdot \mathbf{c}_1)\right)^{-1}. \quad (10)$$

For a uniaxial medium, the tensor takes the following form:

$$\varepsilon = \varepsilon_o + (\varepsilon_e - \varepsilon_o)(\mathbf{c} \cdot \mathbf{c}). \quad (11)$$

For an isotropic medium, the tensor is a diagonal matrix (6).

Note also that the refractive indices depend on the circular frequency ω. In this paper, we do not show explicit dependencies on ω, because all computations and formulas are valid for an arbitrary ω.

It can be seen that for anisotropic media, that is, for media in which at least one of the three principal permittivities differs from the two others, the vectors $\mathbf{D}$ and $\mathbf{E}$ turn out to be noncollinear, which changes considerably the entire electromagnetic wave structure (Fig. 2). The vector of phase propagation $\mathbf{m}$ is proportional to $[\mathbf{DH}]$. The direction of propagation of a ray (energy) is described by the Poynting vector $\mathbf{p}$ proportional to $[\mathbf{EH}]$, and in this case, it does not coincide with the direction of phase propagation. An electromagnetic wave in an anisotropic medium is not strictly transverse, since there exists a nonzero projection of the vector $\mathbf{E}$ onto the direction of phase propagation $\mathbf{m}$.

Consider system (4) in more detail. Excluding the vector $\mathbf{E}$ from it, we obtain

$$\mathbf{E} = \varepsilon^{-1}\mathbf{D} = -\varepsilon^{-1}\mathbf{m}^{\times}\mathbf{H}.$$

Making substitution into the second equation of system (4), we obtain for the components of vector $\mathbf{H}$ the equation

$$(1 + \mathbf{m}^{\times}\varepsilon^{-1}\mathbf{m}^{\times})\mathbf{H} = 0. \tag{12}$$

The equation has nonzero solutions if the matrix determinant is zero [7]:

$$\mathbf{m}^2\ \mathbf{m}\varepsilon\mathbf{m} - \mathbf{m}(\bar{\varepsilon}_t - \bar{\varepsilon})\mathbf{m} + |\varepsilon| = 0. \tag{13}$$

If we substitute the representation $\mathbf{m} = n\mathbf{n}$, we obtain an equation that is biquadratic for n and is known as the Fresnel normal equation for isotropic, uniaxial, and biaxial media:

$$n^4\mathbf{n}\varepsilon\mathbf{n} - n^2\mathbf{n}(\bar{\varepsilon}_t - \bar{\varepsilon})\mathbf{n} + |\varepsilon| = 0.$$

For uniaxial media, taking into account (11), for components of the phase propagation vector, we obtain the equation:

$$(\mathbf{m}^2 - \varepsilon_o)(\mathbf{m}\varepsilon\mathbf{m} - \varepsilon_o\varepsilon_e) = 0.$$

One can see that this equation can be split into two equations. In case of an ordinary ray, for the phase propagation vector $\mathbf{m}_o$, we have

$$\mathbf{m}_o^2 - \varepsilon_o = 0. \tag{14}$$

In case of an extraordinary ray, for the phase propagation vector $\mathbf{m}_e$

$$\mathbf{m}_e\varepsilon\mathbf{m}_e - \varepsilon_o\varepsilon_e = 0. \tag{15}$$

For isotropic media, (13) takes the following form:

$$\mathbf{m}_i^2 - \varepsilon_i = 0. \tag{16}$$

Determine the directions of oscillations of the vectors $\mathbf{E}$ and $\mathbf{H}$ in anisotropic media. For this, we substitute into (12) the representation for tensor (11) and obtain the formula [7]

$$\left(\varepsilon_o - \mathbf{m}^2 + \frac{(\varepsilon_e - \varepsilon_o)}{\varepsilon_e}([\mathbf{mc}] \cdot [\mathbf{mc}])\right)\mathbf{H} = 0.$$

Then, the vector $\mathbf{H}$ for uniaxial media can be represented in the following form:

$$\mathbf{H}_o = A_o\mathbf{h}_o, \tag{17}$$

where $\mathbf{h}_o = [\mathbf{m}_o[\mathbf{m}_o\mathbf{c}]]$,

$$\mathbf{H}_e = A_e\mathbf{h}_e, \tag{18}$$

where $\mathbf{h}_e = [\mathbf{m}_e\mathbf{c}]$. Here, A_o and A_e are real constants and $\mathbf{m}_o$ and $\mathbf{m}_e$ are the phase propagation vectors of ordinary and extraordinary rays, respectively.

For biaxial media, substituting (10) into (12), we have

$$\left(1 - \frac{\mathbf{m}^2}{\varepsilon_2} - \frac{1}{2}\left(\frac{1}{\varepsilon_1} - \frac{1}{\varepsilon_3}\right)var\right)\mathbf{H} = 0,$$

where $var = [\mathbf{mc}_1] \cdot [\mathbf{mc}_2] + [\mathbf{mc}_2] \cdot [\mathbf{mc}_1]$. This equation has two solutions that we call plus-ray and minus-ray to distinguish one solution from another only. The vector $\mathbf{H}$ for biaxial media can be represented in the following form:

$$\mathbf{H}_\pm = A_\pm\mathbf{h}_\pm, \tag{19}$$

where

$$\mathbf{h}_\pm = \sqrt{[\mathbf{m}_\pm\mathbf{c}_2]^2}[\mathbf{m}_\pm\mathbf{c}_1] \pm \sqrt{[\mathbf{m}_\pm\mathbf{c}_1]^2}[\mathbf{m}_\pm\mathbf{c}_2]. \tag{20}$$

Here, A_+ and A_- are the real constants and $\mathbf{m}_+$ and $\mathbf{m}_-$ are the phase propagation vectors of the plus-ray and minus-ray, respectively.

It should be noted that in the case when triple $\mathbf{c}_1, \mathbf{c}_2, \mathbf{m}_\pm$ is coplanar one of vectors $\mathbf{h}_+$ or $\mathbf{h}_-$ is zero (denote it as $\mathbf{h}_{=0}$), it means that the (20) is not working for this case. Another vector $\mathbf{h}_{\neq 0}$ is nonzero and $\mathbf{h}_{\neq 0} \parallel [\mathbf{c}_1\mathbf{c}_2]$. By definition, $\mathbf{m}_\pm\mathbf{h}_\pm = 0$ and $\mathbf{h}_+\mathbf{h}_- = 0$; therefore, $\mathbf{h}_{=0} \parallel [\mathbf{m}[\mathbf{c}_1\mathbf{c}_2]]$. Length and sign of the vector $\mathbf{h}_{=0}$ are unimportant for calculations and it can be taken as $\mathbf{h}_{=0} = [\mathbf{m}[\mathbf{c}_1\mathbf{c}_2]]$.

It follows from the system of equations (4) that $\mathbf{E} = -\varepsilon^{-1}[\mathbf{mH}]$. Hence, we obtain the vector $\mathbf{E}$ for an electromagnetic wave propagating in an anisotropic medium as follows:

$$\mathbf{E}_\beta = A_\beta\mathbf{e}_\beta, \tag{21}$$

where $\mathbf{e}_\beta = -\varepsilon^{-1}[\mathbf{m}_\beta\mathbf{h}_\beta]$ and $\beta \in \{o, e, +, -\}$.

From (17)-(21), it follows that all rays propagating in *transparent* anisotropic media are linearly polarized. Note that in an absorbing medium, the rays are slightly elliptically polarized [8].

The energy flow density ξ of an electromagnetic field is defined as the sum of energies of an electric field ξ_e and a magnetic field ξ_m [7]:

$$\xi = \xi_e + \xi_m, \xi_e = \frac{(Re\mathbf{E})(Re\mathbf{D})}{8\pi}, \xi_m = \frac{(Re\mathbf{H})(Re\mathbf{B})}{8\pi}.$$

From (4), taking into account the fact that the vector $\mathbf{m}$ is real, we obtain

$$\xi = \frac{1}{4\pi}(Re\mathbf{H})^2. \tag{22}$$

The vector of energy flow density (Poynting vector) is determined by the following expression:

$$\mathbf{P} = \frac{c}{4\pi}[Re\mathbf{E}, Re\mathbf{H}]. \tag{23}$$

The ray energy propagation vector is the vector

$$\mathbf{p} = \frac{\mathbf{P}}{c\xi} = \frac{\mathbf{s}}{s}, \tag{24}$$

where $\mathbf{s}$ is the unit vector of ray energy propagation, s is the ray refraction coefficient in the medium, and c is the light speed in vacuum.

Multiplying (23) scalarly by $\mathbf{m}$ and using (4) and (22), we obtain

$$\xi = \frac{1}{c}\mathbf{mP}.$$

And, with allowance for (24),

$$\mathbf{mp} = 1. \tag{25}$$

The phase propagation vector $\mathbf{m}$ will be called *F-normalized* if it satisfies the Fresnel normal equation for the medium in which the wave propagates (13)-(16). In this case, its length is equal to the phase refraction coefficient n, that is, $|\mathbf{m}| = n$. The vector of ray energy propagation will be called *F-normalized* if its length is inverse to the ray energy coefficient of refraction, that is, $|\mathbf{p}| = 1/s$.

For F-normalized vectors $\mathbf{m}$ and $\mathbf{p}$, one can write equations for explicit calculation of $\mathbf{m}$ by using the vector $\mathbf{p}$ and vice versa. For this, it is necessary to include the representations of the vectors $\mathbf{E}$ and $\mathbf{H}$ (17)-(21) into the expression for the Poynting vector (23) and take into account (25). The derivation of corresponding relations, which is rather cumbersome, is omitted (see [7]).

For isotropic media,

$$\mathbf{p}_i = \varepsilon^{-1}\mathbf{m}_i, \tag{26}$$

$$\mathbf{m}_i = \varepsilon\mathbf{p}_i. \tag{27}$$

For uniaxial media,

$$\mathbf{p}_o = \frac{\mathbf{m}_o}{\varepsilon_o}, \mathbf{p}_e = \frac{\varepsilon\mathbf{m}_e}{\varepsilon_o\varepsilon_e}, \tag{28}$$

$$\mathbf{m}_o = \varepsilon_o\mathbf{p}_o, \mathbf{m}_e = \varepsilon^{-1}\mathbf{p}_e\varepsilon_o\varepsilon_e. \tag{29}$$

For biaxial media,

$$\mathbf{p}_\pm = \frac{\mathbf{m}_\pm\varepsilon\mathbf{m}_\pm \cdot \mathbf{m}_\pm + \mathbf{m}_\pm^2 \cdot \varepsilon\mathbf{m}_\pm - (\bar{\varepsilon}_t - \bar{\varepsilon})\mathbf{m}_\pm}{\mathbf{m}_\pm^2 \cdot \mathbf{m}_\pm\varepsilon\mathbf{m}_\pm - |\varepsilon|}, \tag{30}$$

$$\mathbf{m}_\pm = \frac{\mathbf{p}_\pm\varepsilon^{-1}\mathbf{p}_\pm \cdot \mathbf{p}_\pm + \mathbf{p}_\pm^2 \cdot \varepsilon^{-1}\mathbf{p}_\pm - (\overline{\varepsilon^{-1}}_t - \overline{\varepsilon^{-1}})\mathbf{p}_\pm}{\mathbf{p}_\pm^2 \cdot \mathbf{p}_\pm\varepsilon^{-1}\mathbf{p}_\pm - |\varepsilon^{-1}|}. \tag{31}$$

Note that the tensor ε in (26)-(31) is assumed to be the tensors (6)-(8) of the medium where the ray propagates.

Another important characteristic of a ray is its intensity. By definition, ray intensity is the amount of energy it brings per unit area perpendicular to the direction of propagation. The ray intensity is calculated by the following formula [7], [8]:

$$I = |mean(\mathbf{Pq})|, \tag{32}$$

where $\mathbf{P}$ is the Poynting vector, $\mathbf{q}$ is the normal to the surface, and $mean()$ denotes averaging over time, since the radiation receivers record an energy value that is averaged over a time period.

Let us simplify the expressions for each type of media. Since the vectors $\mathbf{H}$ and $\mathbf{E}$ are real in an anisotropic medium, the expression for the Poynting vector (23) is reduced to the following form:

$$\mathbf{P} = \frac{c}{4\pi}[\mathbf{EH}]. \tag{33}$$

Substituting (33) into (32) and taking into account (17)-(21), we obtain for the intensity of a ray propagating in an anisotropic medium:

$$I_\beta = \frac{c}{8\pi}A_\beta^2 U_\beta, \tag{34}$$

where $U_\beta = \left|[\mathbf{e}_\beta\mathbf{h}_\beta]\mathbf{q}\right|$and $\beta \in \{o, e, +, -\}$.

Since the vectors $\mathbf{E}$ and $\mathbf{H}$ in an isotropic medium can be complex, to write a similar equation we represent them as the sum of projections. Let the vector $\mathbf{m}^\perp$ be an arbitrary unit vector perpendicular to the phase propagation direction $\mathbf{m}_i$. Then, $\mathbf{E}$ and $\mathbf{H}$ can be represented as follows:

$$\mathbf{E}_i = A_i\mathbf{m}^\perp + B_i[\mathbf{n}_i\mathbf{m}^\perp], \tag{35}$$

$$\mathbf{H}_i = [\mathbf{m}_i\mathbf{E}_i] = A_i[\mathbf{m}_i\mathbf{m}^\perp] - n_iB_i\mathbf{m}^\perp, \tag{36}$$

where $\mathbf{n}_i$ is the unit vector of ray propagation direction, n_i is the refractive index of the medium, and A_i and B_i are some complex constants. Then, (32) is reduced to the following form:

$$I_i = \frac{c}{8\pi}\left(|A_i|^2 + |B_i|^2\right)U_i, \tag{37}$$

where $U_i = |\mathbf{m}_i\mathbf{q}|$.

5 Model of Interaction of a Ray with the Boundary between Two Media

Some geometrical relations for light reflection and refraction can be obtained from the following conditions of equality of tangential components of the electric field vectors $\mathbf{E}$ and equality of the magnetic field vectors $\mathbf{H}$ [7]:

$$[(\mathbf{E}_1 - \mathbf{E}_2)\ \mathbf{q}] = 0, \tag{38}$$

$$\mathbf{H}_1 - \mathbf{H}_2 = 0. \tag{39}$$

Here, the subscripts denote the medium. When a wave falls onto the boundary between two media, in the general case there appear ν reflected waves and τ refracted waves. In this case, (39) is reduced to the form

$$\mathbf{H}_0 + (\mathbf{H}_{r1} + \cdots + \mathbf{H}_{r\nu}) - (\mathbf{H}_{t1} + \cdots + \mathbf{H}_{t\tau}) = 0.$$

Here, the subscript 0 denotes the incident wave and the subscripts r and t correspond to the reflected and transmitted waves, respectively. With allowance for (3), we obtain

$$\begin{aligned} &\mathbf{H}_0e^{i\phi_0} + \left(\mathbf{H}_{r1}e^{i\phi_{r1}} + \cdots + \mathbf{H}_{r\nu}e^{i\phi_{r\nu}}\right) - \\ &\left(\mathbf{H}_{t1}e^{i\phi_{t1}} + \cdots + \mathbf{H}_{t\tau}e^{i\phi_{t\tau}}\right) = 0. \end{aligned} \tag{40}$$

Let $\gamma \in \{0, r1, \ldots, r\nu, t1, \ldots, t\tau\}$. Since $\phi_\gamma = \omega_\gamma(t - \frac{1}{c}\mathbf{m}_\gamma\mathbf{r})$, (40) must be satisfied at all points of the boundary and at all times, i.e., the wave frequency ω_γ will not change at interaction with the boundary between media and $(\mathbf{m}_\gamma - \mathbf{m}_0)\mathbf{r} = 0$.

Taking into account the fact that the equations are satisfied only at points of the boundary between the media, that is, $\mathbf{rq} = 0$, it follows from the arbitrariness of the radius vector $\mathbf{r}$ that $(\mathbf{m}_\gamma - \mathbf{m}_0)\|\mathbf{q}$. This means that all $\mathbf{m}_\gamma$ end on the same vertical line, see Fig. 3.

Multiplying by the vector $\mathbf{q}$, we obtain $[\mathbf{m}_\gamma\mathbf{q}] = [\mathbf{m}_0\mathbf{q}]$.

Let us introduce vectors $\mathbf{a} = [\mathbf{m}_\gamma\mathbf{q}]$, $\mathbf{g} = [\mathbf{qa}]$, and $\eta_\gamma = \mathbf{m}_\gamma\mathbf{q}$. Then, the phase propagation vector $\mathbf{m}_\gamma$ can be represented as

$$\mathbf{m}_\gamma = \mathbf{g} + \eta_\gamma\mathbf{q}. \tag{41}$$

Since the F-normalized phase propagation vector $\mathbf{m}_0$ of the incident wave is known, we can calculate the vector $\mathbf{g}$:

$$\mathbf{g} = \mathbf{m}_0 - (\mathbf{m}_0\mathbf{q})\mathbf{q}. \tag{42}$$

One can see that the vector $\mathbf{g}$ is the projection of the phase propagation vector $\mathbf{m}_0$ onto the plane Σ, and it is very important that it is *common* for the phase propagation vectors of the incident wave and all generated waves. This is a key fact for obtaining geometrical relations for the interaction of a light ray with the boundary between two

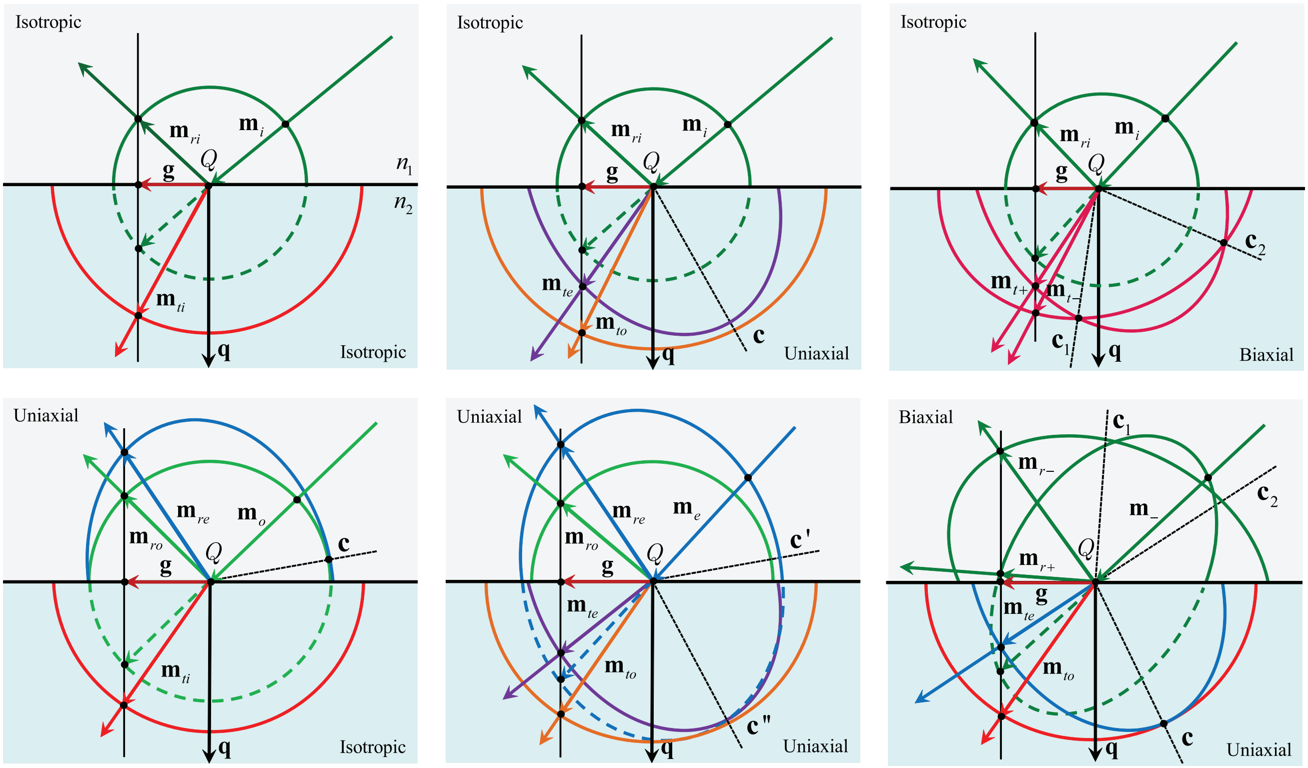

Fig. 3. Several possible combinations of the *first* and the *second* media and different types of an incoming ray. The circumferences and the ellipses in the pictures are sections by the plane Π of decision surfaces of equations (13)-(16) with $\mathbf{m}$ replaced by a radius vector $\mathbf{r}$ from the point Q. Points of intersections (fat dots) of the perpendicular (vertical thin line) with circumferences and ellipses show outgoing phase propagation vectors. The vector $\mathbf{g}$ is a projection of all phase propagation vectors onto the boundary plane Σ. Optical axes of uniaxial media are denoted as $\mathbf{c}, \mathbf{c}', \mathbf{c}''$; for biaxial media: $\mathbf{c}_1, \mathbf{c}_2$. Points of intersections of the optical axes with the circumferences and the ellipses are marked by fat dots if and only if these points lie in the plane Π. Here, the subscripts' letters $i, o, e, +, -$ mark ray types, subscripts r, t are used to distinguish reflected and transmitted rays.

media. It is also important that, as follows from (41), all vectors $\mathbf{m}_\gamma$ lie in one plane, in contrast to the corresponding vectors $\mathbf{p}_\gamma$, see (26)-(31).

To calculate the F-normalized phase propagation vectors for all reflected and refracted rays, substitute (41) into the equations of normals for the first and second media, respectively. If a medium is isotropic, its equation of normals is (16), and then

$$\mathbf{m}_i^2 = (\mathbf{g} + \eta_i \mathbf{q})^2 = \eta_i^2 + 2\eta_i \mathbf{gq} + \mathbf{g}^2 = \varepsilon_i. \tag{43}$$

For a uniaxial medium, we obtain the following equations:

$$\mathbf{m}_o^2 = (\mathbf{g} + \eta_o \mathbf{q})^2 = \eta_o^2 + 2\eta_o \mathbf{gq} + \mathbf{g}^2 = \varepsilon_o, \tag{44}$$

and

$$\mathbf{m}_e \varepsilon \mathbf{m}_e = \eta_e^2 \mathbf{q}\varepsilon\mathbf{q} + 2\eta_e(\mathbf{g}\varepsilon\mathbf{q}) + \mathbf{g}\varepsilon\mathbf{g} = \varepsilon_o \varepsilon_e. \tag{45}$$

If a medium is biaxial, substitution of (41) into its equation of normals (13) yields

$$(\mathbf{g} + \eta_\pm \mathbf{q})^2 \cdot (\mathbf{g} + \eta_\pm \mathbf{q})\varepsilon(\mathbf{g} + \eta_\pm \mathbf{q}) - (\mathbf{g} + \eta_\pm \mathbf{q})(\bar{\varepsilon}_t - \bar{\varepsilon})(\mathbf{g} + \eta_\pm \mathbf{q}) + |\varepsilon| = 0.$$

Opening the brackets, we obtain the following equation of the fourth kind [7]:

$$A\eta_\pm^4 + B\eta_\pm^3 + C\eta_\pm^2 + D\eta_\pm + F = 0, \tag{46}$$

where $A = \mathbf{q}\varepsilon\mathbf{q}$, $B = 2\mathbf{g}\varepsilon\mathbf{q}$, $C = \mathbf{g}\varepsilon\mathbf{g} + \mathbf{g}^2\mathbf{q}\varepsilon\mathbf{q} - \mathbf{q}(\bar{\varepsilon}_t - \bar{\varepsilon})\mathbf{q}$, $D = 2(\mathbf{g}^2(\mathbf{g}\varepsilon\mathbf{q}) + \mathbf{g}\bar{\varepsilon}\mathbf{q})$, $F = \mathbf{g}^2(\mathbf{g}\varepsilon\mathbf{g}) - \mathbf{g}(\bar{\varepsilon}_t - \bar{\varepsilon})\mathbf{g} + |\varepsilon|$.

Solving (43)-(46) (for both media), in the general case we obtain up to eight complex values η_β (for the boundary between two anisotropic media: four roots for each medium). For each value η_β, where $\beta \in \{i, o, e, +, -\}$, by (41) we calculate the vector $\mathbf{m}_\beta$. Using (26), (28), and (30), which depend on the medium type, we calculate the vector $\mathbf{p}_\beta$ for each vector $\mathbf{m}_\beta$.

For all really existing reflected and refracted rays, their phase propagation vectors $\mathbf{m}$ and the corresponding vectors $\mathbf{p}$ are real; here, $\mathbf{pq} < 0$ for reflected rays and $\mathbf{pq} > 0$ for refracted rays. It should be noted that a situation when $\mathbf{pq} > 0$ and $\mathbf{mq} < 0$ and vice versa is not contradictory. According to these two criteria (reality of the vector $\mathbf{m}$ and the sign of $\mathbf{pq}$), only those rays are selected that really exist and are classified as reflected and refracted ones.

For each of the generated rays, it is necessary to determine its type: isotropic, ordinary, extraordinary, plus-ray, or minus-ray. The determination of the first three types is evident, because they result from solving three different equations (43)-(46). In the case of a biaxial medium to understand whether the ray is a plus or a minus one, it is necessary to calculate its wave coefficient of refraction, that is, $n = |\mathbf{m}|$. Accordingly to [7],

$$\varepsilon_1 \le n_+^2 \le \varepsilon_2 \le n_-^2 \le \varepsilon_3. \tag{47}$$

Another problem is that of obtaining amplitude relations between the incident ray and generated rays. For this, it is necessary to resolve the system of equations (38), (39) using the calculated phase propagation vectors $\mathbf{m}_\gamma$ and the representation of the vectors $\mathbf{E}$ and $\mathbf{H}$ for each of the media: (19)-(21) for biaxial media, (17), (18), and (21) for uniaxial media, and (35) and (36) for isotropic media. Since in (35) and (36), the vector $\mathbf{m}^{\perp}$ is an arbitrary unit vector perpendicular to the direction of phase propagation, that is, to the vector $\mathbf{m}_\gamma$, we set $\mathbf{m}^{\perp} = \mathbf{u}$. Then, system (35), (36) takes the following form:

$$\mathbf{E}_i = A_i\mathbf{u} + B_i[\mathbf{n}_i\mathbf{u}], \tag{48}$$

$$\mathbf{H}_i = A_i[\mathbf{m}_i\mathbf{u}] - n_iB_i\mathbf{u}. \tag{49}$$

Then, (38) and (39) are reduced to the following form:

$$[(\mathbf{E}_0 + (\mathbf{E}_{r1} + \cdots + \mathbf{E}_{r\nu}) - (\mathbf{E}_{t1} + \cdots + \mathbf{E}_{t\tau}))\ \mathbf{q}] = 0,$$

$$\mathbf{H}_0 + (\mathbf{H}_{r1} + \cdots + \mathbf{H}_{r\nu}) - (\mathbf{H}_{t1} + \cdots + \mathbf{H}_{t\tau}) = 0.$$

It is important that this system contains all phase propagation vectors including complex-valued ones for refracted rays and reflected rays. Rearranging the elements relating to the incident wave to the right-hand side of the equation, we obtain

$$\begin{aligned}&([\mathbf{E}_{t1}\mathbf{q}] + \cdots + [\mathbf{E}_{t\tau}\mathbf{q}])\\ &\quad - ([\mathbf{E}_{r1}\mathbf{q}] + \cdots + [\mathbf{E}_{r\nu}\mathbf{q}]) = [\mathbf{E}_0\mathbf{q}],\end{aligned} \tag{50}$$

$$(\mathbf{H}_{t1} + \cdots + \mathbf{H}_{t\tau}) - (\mathbf{H}_{r1} + \cdots + \mathbf{H}_{r\nu}) = \mathbf{H}_0. \tag{51}$$

To solve system (50) and (51), substitute the representations of the vectors $\mathbf{E}$ and $\mathbf{H}$ (17)-(21), (48), (49) into it and multiply scalarly each equation by two arbitrary perpendicular vectors lying in the plane Σ (we use the vectors $\mathbf{u}$ and $\mathbf{v}$). Taking into account the fact that $\mathbf{v} = [\mathbf{qu}]$ and $\mathbf{u} = [\mathbf{vq}]$, see Fig. 1, we obtain the following system of four equations:

$$(\mathbf{E}_{t1}\mathbf{u} + \cdots + \mathbf{E}_{t\tau}\mathbf{u}) - (\mathbf{E}_{r1}\mathbf{u} + \cdots + \mathbf{E}_{r\nu}\mathbf{u}) = \mathbf{E}_0\mathbf{u}, \tag{52}$$

$$(\mathbf{E}_{t1}\mathbf{v} + \cdots + \mathbf{E}_{t\tau}\mathbf{v}) - (\mathbf{E}_{r1}\mathbf{v} + \cdots + \mathbf{E}_{r\nu}\mathbf{v}) = \mathbf{E}_0\mathbf{v}, \tag{53}$$

$$(\mathbf{H}_{t1}\mathbf{u} + \cdots + \mathbf{H}_{t\tau}\mathbf{u}) - (\mathbf{H}_{r1}\mathbf{u} + \cdots + \mathbf{H}_{r\nu}\mathbf{u}) = \mathbf{H}_0\mathbf{u}, \tag{54}$$

$$(\mathbf{H}_{t1}\mathbf{v} + \cdots + \mathbf{H}_{t\tau}\mathbf{v}) - (\mathbf{H}_{r1}\mathbf{v} + \cdots + \mathbf{H}_{r\nu}\mathbf{v}) = \mathbf{H}_0\mathbf{v}. \tag{55}$$

Since the terms in the right-hand sides of the equations are determined by the incident wave, they are assumed to be known. Solve the system for the variables A_γ and B_γ, where $\gamma \in \{r1, \ldots, r\nu, t1, \ldots, t\tau\}$. The system turns out to be uniquely solvable only if the number of free variables equals to the number of equations. If an isotropic ray (that is, a ray propagating in an isotropic medium) participates in the interaction with the boundary, there are two free variables in the system (52)-(55). For a linearly polarized ray propagating in an anisotropic medium, there is one free variable. This is realistic, because the number of rays generated by the interaction and their types must be such that the number of free variables is strictly equal to 4. When a ray falls on the boundary between two anisotropic media, in the general case, there form four linearly polarized rays; at the boundary between two isotropic media, there form two isotropic rays; and at the boundary between an isotropic medium and an anisotropic one, there form two linearly polarized rays and one isotropic ray. Thus, in any case four free variables are found, and the equation is uniquely solvable.

Let us consider an example of setting up such an equation. When a ray falls from an isotropic medium onto the boundary with a uniaxial medium, we obtain the following system of equations:

$$([\mathbf{E}_o\mathbf{q}] + [\mathbf{E}_e\mathbf{q}]) - [\mathbf{E}_r\mathbf{q}] = [\mathbf{E}_0\mathbf{q}], \tag{56}$$

$$(\mathbf{H}_o + \mathbf{H}_e) - \mathbf{H}_r = \mathbf{H}_0. \tag{57}$$

Here, the subscripts o, e, r, and 0 denote ordinary refracted, extraordinary refracted, isotropic reflected, and isotropic incident ray, respectively.

Let the refractive index of an isotropic medium be n. Substituting the corresponding representations ((17)-(21) or (48), (49)) of vectors $\mathbf{E}$ and $\mathbf{H}$, we obtain

$$\begin{aligned}&(A_o[\mathbf{e}_o\mathbf{q}] + A_e[\mathbf{e}_e\mathbf{q}]) - (A_r[\mathbf{uq}] + B_r[[\mathbf{n}_r\mathbf{u}]\mathbf{q}])\\ &\quad = A_0[\mathbf{uq}] + B_0[[\mathbf{n}_0\mathbf{u}]\mathbf{q}],\end{aligned} \tag{58}$$

$$\begin{aligned}&(A_o\mathbf{h}_o + A_e\mathbf{h}_e) - (A_r[\mathbf{m}_r\mathbf{u}] - B_r(n\mathbf{u}))\\ &\quad = A_0[\mathbf{m}_0\mathbf{u}] - B_0(n\mathbf{u}).\end{aligned} \tag{59}$$

Multiplying both equations by $\mathbf{u}$ and $\mathbf{v}$ and the thus obtaining system of four equations, we obtain the quantities A_o, A_e, A_r, and B_r. Hence, we can calculate the vectors $\mathbf{E}$ and $\mathbf{H}$ for all reflected and refracted rays ((17)-(21) or (48), (49)).

Since system (52)-(55) can be set up and solved for the boundary of two media, the problem of calculating the parameters of reflected and refracted rays can be fully solved.

Remark. It should be noted that in this paper the changes in the phase between the incident wave and generated waves are not considered.

6 Representation of Light Polarization

In this paper, to present light polarization, we chose an approach based on coherence matrices and their modifiers [9], [8]. Give a brief description of this approach needed for the algorithm.

Introduce a Cartesian system of coordinates connected with a ray, with a basis $\{\mathbf{x}, \mathbf{y}, \mathbf{z}\}$. The vector $\mathbf{z}$ is directed toward the ray propagation. Then, the complex Jones vector is [9]

$$\tilde{\mathbf{E}} = \begin{pmatrix}\tilde{E}_x\\ \tilde{E}_y\end{pmatrix} = \begin{pmatrix}E_xe^{i(\omega t+\delta_x)}\\ E_ye^{i(\omega t+\delta_y)}\end{pmatrix},$$

where ω is the circular frequency, δ_x and δ_y are the initial oscillation phases, E_x and E_y are the amplitudes of projection of the vector $\mathbf{E}$ onto the vectors $\mathbf{x}$ and $\mathbf{y}$, respectively. A real part of the electric field vector $\mathbf{E}$ is $Re\tilde{\mathbf{E}}$. A complex matrix of the form [9]

$$J = \langle\tilde{\mathbf{E}} \times \tilde{\mathbf{E}}^\dagger\rangle = \begin{pmatrix}\langle\tilde{E}_x\tilde{E}_x^*\rangle & \langle\tilde{E}_x\tilde{E}_y^*\rangle\\ \langle\tilde{E}_y\tilde{E}_x^*\rangle & \langle\tilde{E}_y\tilde{E}_y^*\rangle\end{pmatrix} = \begin{pmatrix}J_{xx} & J_{xy}\\ J_{yx} & J_{yy}\end{pmatrix}$$

is called the coherence matrix. Here $(\bullet)^*$ denotes complex conjugation, $\langle\bullet\rangle$ is mathematical expectation, and $(\bullet)^\dagger$ the transposition and complex conjugation. The coherence matrix with the system of coordinates $\{\mathbf{x}, \mathbf{y}, \mathbf{z}\}$ connected with the ray fully describes the state of ray polarization.

The diagonal elements of the matrix J are real and represent the intensities of the x- and y-components, respectively. The ray intensity is equal to the trace of the matrix J:

$$I = J_{xx} + J_{yy} = \langle \tilde{E}_x \tilde{E}_x^* \rangle + \langle \tilde{E}_y \tilde{E}_y^* \rangle. \quad (60)$$

Let the electric field of the ray change as $\tilde{\mathbf{E}}' = M\tilde{\mathbf{E}}$, where M is a complex matrix describing the change of the electric field. Then, the new coherence matrix J' is calculated as

$$J' = \langle \tilde{\mathbf{E}} \times \tilde{\mathbf{E}}'^{\dagger} \rangle = \langle M\tilde{\mathbf{E}} \times \tilde{\mathbf{E}}^{\dagger} M^{\dagger} \rangle = MJM^{\dagger}. \quad (61)$$

The matrix M is called the matrix modifier of the coherence matrix. Expression (61) defines the rule for applying the matrix modifier to the coherence matrix.

In this paper, for convenient calculations, we use a special systems of coordinates for each ray. For an anisotropic medium, the ray is linearly polarized. Then, we have (see (17)-(21)):

$$\mathbf{x} = \frac{\mathbf{e}_\beta}{|\mathbf{e}_\beta|}, \mathbf{y} = \frac{\mathbf{h}_\beta}{|\mathbf{h}_\beta|}, \mathbf{z} = \frac{\mathbf{p}_\beta}{|\mathbf{p}_\beta|}, \quad (62)$$

where $\beta \in \{o, e, +, -\}$. For an isotropic medium, since it does not have a special direction and the ray is arbitrary polarized, this system of coordinates can be defined only at the boundary between the media (see (48), (49)), namely:

$$\mathbf{x} = \mathbf{u}, \mathbf{y} = [\mathbf{nu}], \mathbf{z} = \mathbf{n}. \quad (63)$$

At the point of interaction (Q in Fig. 1), the system of coordinates connected with the ray must be rotated. Let the system $\{\mathbf{x}, \mathbf{y}, \mathbf{z}\}$ be connected with the generated ray and the system $\{\mathbf{x}', \mathbf{y}', \mathbf{z}\}$ be connected with the incident ray. To recalculate the coherence matrix, one can use the following matrix modifier:

$$M_{rotate} = \begin{pmatrix} \mathbf{xx}' & \mathbf{yx}' \\ \mathbf{xy}' & \mathbf{yy}' \end{pmatrix}. \quad (64)$$

7 Algorithm to Calculate the Interaction of a Ray with the Boundary between Two Media

This section is devoted to a description of an algorithm to calculate the interaction of a ray with the boundary between two arbitrary nonmagnetic transparent media. Let

$$R = \{r_0, \mathbf{r}_d, \mathbf{m}, J, CS, TP, \lambda, FN\} \quad (65)$$

be called a ray. Here, r_0 is the initial point of the ray, $\mathbf{r}_d$ is the unit vector of ray propagation direction, $\mathbf{m}$ is the phase propagation direction, λ is the ray wavelength in vacuum (it uniquely determines the circular frequency ω), J is the coherence matrix of the ray, CS is the system of coordinates connected with the ray, TP is the ray type (isotropic, ordinary, extraordinary, plus, or minus ray), and Boolean FN is true if the ray is F-normalized.

Let the ray R fall on the boundary of two media. It is necessary to calculate the parameters of all reflected and refracted rays. Let the quantities in (65) for the generated ray be denoted by superscript "*."

The algorithm consists of the following steps:

1. *F-normalize the incident ray.* This step must be proceeded only if FN is false.
   a. From (27), (29), and (31), calculate the direction of the phase propagation vector $\mathbf{m}'$ using the direction of the ray $\mathbf{r}_d$ as $\mathbf{p}$. The vector $\mathbf{m}'$ will be parallel to $\mathbf{m}$ and not-F-normalized.
   b. To F-normalize $\mathbf{m}'$, we substitute $\kappa\mathbf{m}'$ into (13)-(16) for the first medium and incident ray type TP as $\mathbf{m}$, and solve it for κ. The equation has several roots, but only one is real and positive, we should select it as κ value. Then, $\mathbf{m} = \kappa\mathbf{m}'$.
   c. Recall relation (25). Then, the ray energy propagation vector $\mathbf{p} = \frac{\mathbf{r}_d}{\mathbf{mr}_d}$.
2. *Transform the ray coherence matrix* to a system of coordinates needed for calculations. Depending on the medium, the type of ray TP, and the boundary at which the interaction is calculated, we formulate the needed system of coordinates (62), (63). Applying the matrix-modifier (64) according to (61), we transform the coherence matrix to a new system of coordinates.
3. *Calculate the projection* $\mathbf{g}$ of the vector $\mathbf{m}$ of the incident ray in the plane of the boundary Σ by (42).
4. *Calculate the vectors* $\mathbf{m}^*$ *for reflected and refracted rays.* Analytically solving equations of normals (43)-(46) for the first and the second media for the η, we obtain a set of η^*. Then, calculate vectors $\mathbf{m}^*$ using (41).
5. *Select vectors* $\mathbf{m}^*$ *and calculate vectors* $\mathbf{p}^*$.
   a. For each real vector $\mathbf{m}^*$, using (26), (28), (30) calculate the vector $\mathbf{p}^*$. Choose such vectors $\mathbf{m}^*$ for which one of the following conditions is satisfied:
      i. $\mathbf{p}^*\mathbf{q} > 0$ for refracted rays, i.e., the vector $\mathbf{m}^*$ is obtained from the equation of normals for the second medium,
      ii. $\mathbf{p}^*\mathbf{q} < 0$ for reflected rays, i.e., the vector $\mathbf{m}^*$ is obtained from the equation of normals for the first medium.
   b. From each pair of complex vectors $\mathbf{m}^*$, corresponding to complex-conjugate values η^*, select one of the vectors (any).
6. *Assign the necessary type* TP^* for generated rays depending on the equation used in step 4.
7. *Set up the amplitude equation and solve it.* For each of the calculated phase propagation vectors $\mathbf{m}^*$, form the coefficients of the amplitude equation (see (52)-(55) and explanations to them). The following algorithm can be used to form the equation:
   a. Using (17)-(21), for all generated rays propagating in an anisotropic medium, form one coefficient-column of the following form:

$$\begin{pmatrix} \mathbf{X}_\beta \\ \mathbf{Y}_\beta \end{pmatrix} = \begin{pmatrix} \mathbf{e}_\beta \\ \mathbf{h}_\beta \end{pmatrix},$$

   where $\beta \in \{o, e, +, -\}$.

   Using (48), (49) for all generated rays propagating in an isotropic medium, form two coefficients-columns of the following form:

$$\begin{pmatrix} \mathbf{X}_1 \\ \mathbf{Y}_1 \end{pmatrix} = \begin{pmatrix} \mathbf{u} \\ [\mathbf{m}_i\mathbf{u}] \end{pmatrix}$$
$$\begin{pmatrix} \mathbf{X}_2 \\ \mathbf{Y}_2 \end{pmatrix} = \begin{pmatrix} [\mathbf{n}_i\mathbf{u}] \\ -n_i\mathbf{u} \end{pmatrix}.$$

b. According to the system of equations (50), (51), take coefficients columns for refracted rays with positive signs, and for reflected rays with negative signs and form a 2×4 matrix (two rows, four columns) corresponding to the left-hand side of the system of equations (50), (51).
c. Similarly, form one or two coefficients columns for the incident ray, and form the right-hand side of the matrix of the equation.
d. As a result, obtain a 2×5 matrix if the first medium is anisotropic; 2×6 if it is isotropic.
e. Multiplying each row by $\mathbf{u}$, $\mathbf{v}$ scalarly, obtain a 4×5 (or 4×6) matrix of the amplitude equation.
f. To solve the equation, transform it so that a 4×4 unit matrix is formed in its left-hand side.

Let us apply the consideration to the example shown above (56)-(59). For refracted ordinary and extraordinary rays, we obtain the following coefficients columns (see (17)-(21)):

$$\begin{pmatrix} \mathbf{X}_o \\ \mathbf{Y}_o \end{pmatrix} = \begin{pmatrix} \mathbf{e}_o \\ \mathbf{h}_o \end{pmatrix}$$

and

$$\begin{pmatrix} \mathbf{X}_e \\ \mathbf{Y}_e \end{pmatrix} = \begin{pmatrix} \mathbf{e}_e \\ \mathbf{h}_e \end{pmatrix}.$$

For the reflected ray,

$$\begin{pmatrix} \mathbf{X}_{r1} \\ \mathbf{Y}_{r1} \end{pmatrix} = \begin{pmatrix} \mathbf{u} \\ [\mathbf{m}_r\mathbf{u}] \end{pmatrix}, \begin{pmatrix} \mathbf{X}_{r2} \\ \mathbf{Y}_{r2} \end{pmatrix} = \begin{pmatrix} [\mathbf{n}_r\mathbf{u}] \\ -n\mathbf{u} \end{pmatrix}.$$

For the incident ray,

$$\begin{pmatrix} \mathbf{X}_{01} \\ \mathbf{Y}_{01} \end{pmatrix} = \begin{pmatrix} \mathbf{u} \\ [\mathbf{m}_0\mathbf{u}] \end{pmatrix}, \begin{pmatrix} \mathbf{X}_{02} \\ \mathbf{Y}_{02} \end{pmatrix} = \begin{pmatrix} [\mathbf{n}_0\mathbf{u}] \\ -n\mathbf{u} \end{pmatrix}.$$

The following 2×6 matrix is built from the columns:

$$\begin{pmatrix} \mathbf{X}_o & \mathbf{X}_e & -\mathbf{X}_{r1} & -\mathbf{X}_{r2} & \mathbf{X}_{01} & \mathbf{X}_{02} \\ \mathbf{Y}_o & \mathbf{Y}_e & -\mathbf{Y}_{r1} & -\mathbf{Y}_{r2} & \mathbf{Y}_{01} & \mathbf{Y}_{02} \end{pmatrix}.$$

And finally the required construction is as follows:

$$\begin{pmatrix} \mathbf{X}_o\mathbf{u} & \mathbf{X}_e\mathbf{u} & -\mathbf{X}_{r1}\mathbf{u} & -\mathbf{X}_{r2}\mathbf{u} & \mathbf{X}_{01}\mathbf{u} & \mathbf{X}_{02}\mathbf{u} \\ \mathbf{X}_o\mathbf{v} & \mathbf{X}_e\mathbf{v} & -\mathbf{X}_{r1}\mathbf{v} & -\mathbf{X}_{r2}\mathbf{v} & \mathbf{X}_{01}\mathbf{v} & \mathbf{X}_{02}\mathbf{v} \\ \mathbf{Y}_o\mathbf{u} & \mathbf{Y}_e\mathbf{u} & -\mathbf{Y}_{r1}\mathbf{u} & -\mathbf{Y}_{r2}\mathbf{u} & \mathbf{Y}_{01}\mathbf{u} & \mathbf{Y}_{02}\mathbf{u} \\ \mathbf{Y}_o\mathbf{v} & \mathbf{Y}_e\mathbf{v} & -\mathbf{Y}_{r1}\mathbf{v} & -\mathbf{Y}_{r2}\mathbf{v} & \mathbf{Y}_{01}\mathbf{v} & \mathbf{Y}_{02}\mathbf{v} \end{pmatrix}.$$

It is a form of the system of equations (52)-(55)

$$\begin{aligned} &(M_1\ M_2\ M_3\ M_4)(A_o\ A_e\ A_r\ B_r)^T \\ &\quad = (M_5\ M_6)(A_0\ B_0)^T, \end{aligned} \tag{66}$$

where M_i is the ith column of the construction.

8. *Calculate the coherence matrices for all reflected and refracted rays.* For this, calculate the corresponding matrices modifiers and then apply them according to (61) to the coherence matrix of the incident ray.

a. Nullify the matrix modifier M_D.
b. Copy the elements from the fifth and sixth columns (if the sixth column is available) of the construction to the matrix modifier from the row with the number that is equal to the number of the first coefficient column in the left-hand side of the construction (in columns 1-4) corresponding to the generated ray. The number of copied rows is equal to the number of coefficients columns in the equation corresponding to the generated ray (one row for a ray propagating in an anisotropic medium, and two rows for an isotropic ray). Apply the thus calculated matrix modifier to the coherence matrix of the incident ray as follows:

$$J' = M_D J M_D^{\dagger}. \tag{67}$$

c. To remain (60) valid in any medium, multiply the coherence matrix J' by the coefficient of transmission or reflection not taking into account the amplitude coefficient of the vectors $\mathbf{E}$ and $\mathbf{H}$, because they are taken into account in transformation (67). Denote this coefficient by f, then from (34), (37), we obtain

$$f = \frac{U_\alpha}{U_\beta},$$

where β corresponds to the incident ray, and α corresponds to the outgoing ray.
d. Then, $J^* = fJ'$ is the coherence matrix of the generated ray.

For the boundary between isotropic and uniaxial media, the construction built in the step 7 is transformed to

$$\begin{pmatrix} 1 & 0 & 0 & 0 & M_{15} & M_{16} \\ 0 & 1 & 0 & 0 & M_{25} & M_{26} \\ 0 & 0 & 1 & 0 & M_{35} & M_{36} \\ 0 & 0 & 0 & 1 & M_{45} & M_{46} \end{pmatrix}.$$

It is the solution for the system (66), since

$$\begin{aligned} &(A_o\ A_e\ A_r\ B_r)^T \\ &\quad = (M_1\ M_2\ M_3\ M_4)^{-1}(M_5\ M_6)(A_0\ B_0)^T \\ &\quad = \begin{pmatrix} M_{15} & M_{16} \\ M_{25} & M_{26} \\ M_{35} & M_{36} \\ M_{45} & M_{46} \end{pmatrix} \begin{pmatrix} A_0 \\ B_0 \end{pmatrix}. \end{aligned}$$

Then, matrices modifiers for the ordinary, extraordinary, and reflected rays are equal to

$$M_{Do} = \begin{pmatrix} M_{15} & M_{16} \\ 0 & 0 \end{pmatrix}, M_{De} = \begin{pmatrix} M_{25} & M_{26} \\ 0 & 0 \end{pmatrix},$$
$$M_{Dr} = \begin{pmatrix} M_{35} & M_{36} \\ M_{45} & M_{46} \end{pmatrix}.$$

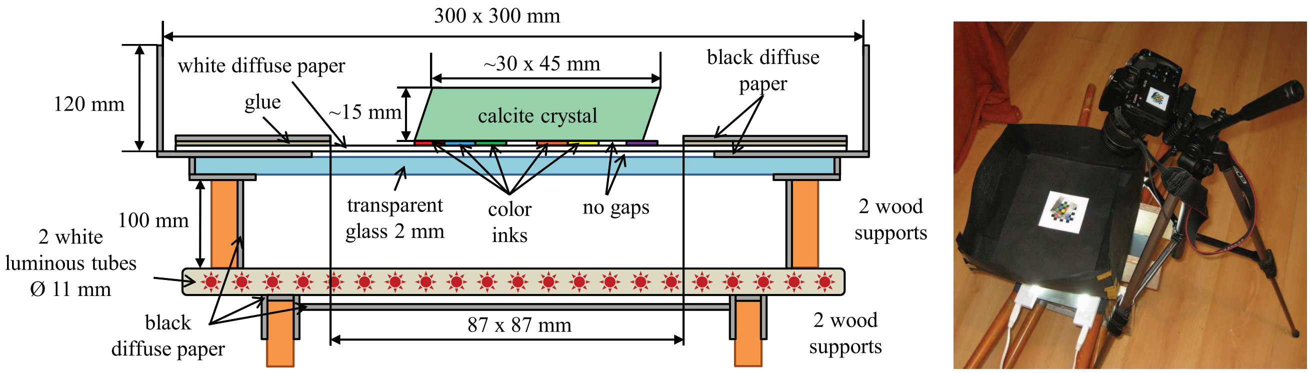

Fig. 4. Left: A detailed scheme of the real scene. Right: a photo of the scene including the photo camera.

Fig. 5. A photo of the real scene with calcite crystal on the left, a simulation in the center, and a pixel-by-pixel difference between the photo and the computed image on the right.

For each ray, we calculate as follows:

$$f_e = \left|\frac{[\mathbf{e}_e\mathbf{h}_e]\mathbf{q}}{\mathbf{m}_0\mathbf{q}}\right|, f_o = \left|\frac{[\mathbf{e}_o\mathbf{h}_o]\mathbf{q}}{\mathbf{m}_0\mathbf{q}}\right|, f_r = \left|\frac{\mathbf{m}_r\mathbf{q}}{\mathbf{m}_0\mathbf{q}}\right| = 1.$$

9. *Calculate and establish the system of coordinates* for each of the generated rays (see (62), (63)).
10. *Set ray properties* for each of the generated rays, $r_0^* = Q$ (the intersection of the ray with the boundary of media) and $\mathbf{r}_d^* = \mathbf{p}^*$. Also set FN^* to true, because $\mathbf{p}^*$ and $\mathbf{m}^*$ are F-normalized.
11. *Stop.*

8 Experiments

One way to validate an algorithm of photorealistic rendering is a comparison of a photograph with a computed image of an analogous virtual scene. The best result of validation is obtained when a photograph and a computed image coincide pixel by pixel. In particular, this approach was applied in [2], [10], [11]. In all cases, the authors encountered a lot of problems, e.g., coincidence of parameters of real and virtual scenes. Nevertheless, it is a useful approach that confirms the validity acceptable for the purposes of realistic computer graphics.

Consider a simple scene including a transparent monocrystal of calcite (Iceland spar) with strong birefringence, see Fig. 5 on the left. The crystal lies on a plane light source similar to an illuminating vitrage with sharp boundaries between colors. This allows making visible birefringence. It is easy to construct such a real scene and a corresponding computer model.

On the right in Fig. 4, the test environment including the arrangement of a real scene and a camera is demonstrated. A scheme of the real scene and its approximate sizes are shown on the left in Fig. 4. The crystal is a convex polyhedron faceted without rounds. It lies on a sheet of white paper with a printed colored texture. The sheet is put on a transparent glass plate and covered by a sheet of black paper with a rectangular window. Two cylindrical luminescent lamps are placed under the plate in such a way as to provide an approximately uniform illumination of the sheet. Other light sources are absent. Specifically, a window with a printed texture and lamps determine the geometrical shape and spectrum of the light source. A camera Canon 450D with lens EF-S 18-55 mm F:3.5-5.6 IS is mounted on a tripod (see Fig. 4 (right)). A minimal matrix sensitivity of ISO100 was selected to decrease noise. To minimize the lens's aperture, the focal number was set to a maximal value of F:36. The exposition should be considerably longer than the period of lamp blinking. The photograph on the left of Fig. 5 is obtained with an exposition equal to 13 seconds.

A virtual scene of a rectangular textured light source and a convex polyhedron (crystal) is placed above at the minimal distance that is sufficient to omit errors in geometric calculations. The real scene air is substituted by vacuum in the virtual scene. The crystal is represented as a set of six faces whose geometrical shapes are similar to the shapes of the real crystal. The crystal geometry was recovered with the following steps:

1. each crystal face was scanned;
2. in each of the scanned images, the pixels that approximately match the polyhedron vertices were marked;
3. two-dimensional geometry of all faces was recovered;
4. three-dimensional geometry of the crystal was recovered.

The optical characteristics of the polyhedron are those of calcite. To determine the direction of the optical axis, two points belonging to large opposite faces of the crystal were selected so that they look like a single point if the observer could see through the crystal. During the recovery of three-dimensional geometry, the optical axis was detected from projections of these points. The virtual camera is a basic pinhole model as in [12]. The determination of camera parameters (camera calibration) was fulfilled manually with the help of an interactive application.

There were problems of coincidence of the spectra of a real and virtual textures:

1. the spectrum of the lamps being used is usually unknown;
2. the spectra of transmittance of the paper and inks are unknown;
3. the lens adds some unknown distortions to the spectrum of transmitted light;
4. the sensitivity of the camera matrix to different parts of the spectrum is unknown too.

To decrease the difference between the colors of textures in the photo and the computed image, the colors of the virtual texture were taken from a blurred (unfocused) photograph of the real texture made with the same camera parameters and exposition. We use RGB data for textures and Glassner's method [13] to choose a plausible spectrum associated with the RGB triple.

A photograph of the real scene is on the left in Fig. 5, and the computed image in the center of Fig. 5. The image was calculated with light backward recursive ray tracing, and ray paths were broken after 15 bounces. On the right in Fig. 5, the absolute difference between the photograph and the computed image is shown. A visual comparison of the pictures in Fig. 5 allows us to conclude that the above-proposed algorithm works quite well. The visible differences may be caused by many reasons. First, the parameters of the real and virtual cameras differ, since an ideal coincidence is practically impossible by using manual fitting. One can see this by comparing the images in [2], [10], [11]. For *transparent* monocrystals, the manual fitting is more laborious because a slight change in the camera parameters causes great changes in the image. This is clearly visible in the images of back faces (visible through front faces). Second, there exists a small difference between the real and virtual crystal geometries. This is because the crystal vertices are slightly blurred or absent at all on the scanned images since the very tips of crystal corners may crumble. Third, the texels of the real and virtual textures may differ because of an irregular paper structure. One can see this on the left in Fig. 5.

The results of a general test of the algorithm are shown in Fig. 6 and concern to rendering of a set of cubes made of isotropic, uniaxial, and biaxial monocrystals and crystalline aggregates. All scenes consist of an axes-aligned cube (min: (0, 0, 0), max: (1.6, 1.6, 1.6)) placed on a square axes-aligned textured plate (min: $(-0.842, -0.842, 0)$, max: (2.484, 2.484, 0)) in a gray light environment ($0.4 \times$ CIE D65). The texture has resolution 41×41 pixels and is white (CIE D65) except a central black cross of 1-pixel width. The coordinate system of all scenes is the same, it is shown in two top rows of images. Main refractive indices are linearly changed from 380 to 780 nm. Directions of the optical axes (binormals) for biaxial media depend on wavelength, but tensor coordinate system is constant (we consider orthorhombic crystal in the test), so we specify a tensor basis. Ray tracing depth for the presented images is nine bounces.

Top row pinhole camera parameters: focus length is 2.62223, aperture point is (0.8, 0.8, -2.70031), view direction is (0, 0, 1), up vector is (0, -1, 0). The camera parameters for the middle and bottom rows: focus length is 8.45695, aperture point is $(4.49411, -3.05049, -12.9591)$, view direction is $(-0.243515, 0.243461, 0.938844)$, up vector is $(-0.0974902, -0.969224, 0.226053)$. Image plane sizes are 4.36×2.18.

For the top and middle rows: isotropic: $n_i \in [1.52; 1.48]$; uniaxial: $n_o = n_i$, $n_e \in [1.75; 1.65]$, $\mathbf{c} = (1, 1, 1)$. Biaxial:

$$\begin{aligned} &n_1 = n_o, n_2 = n_e, n_3 \in [1.92; 1.88], \\ &\mathbf{a}_1 = (0.40825, 0.40825, 0.81650), \\ &\mathbf{a}_2 = (0.57735, 0.57735, -0.57735), \\ &\mathbf{a}_3 = (-0.70711, 0.70711, 0). \end{aligned}$$

The optical axes are shown in the images. In the biaxial case, two binormals for wavelengths of violet ($\mathbf{c}_1^{380}$, $\mathbf{c}_2^{380}$) and red ($\mathbf{c}_1^{780}$, $\mathbf{c}_2^{780}$) light are shown.

For the bottom row: The cubes consist of two half-cubes spitted by a plane $z = 0.8$. Top half-cubes (nearest to the camera) have the same optical properties as monocrystals (in the first two rows). Bottom half-cubes have the following properties: isotropic $n_i \in$ [1.45; 1.35]; uniaxial: $n_o = n_i$, $n_e \in$ [1.55; 1.45], $\mathbf{c} = (-1, 3, 2)$. Biaxial: $n_1 = n_o$, $n_2 = n_e$, $n_3 \in$ [1.65; 1.55], $\mathbf{a}_1 = (0.83909, -0.24328, 0.48656)$, $\mathbf{a}_2 = (0.43402, 0.83862, -0.32917)$, $\mathbf{a}_3 = (-0.32796, 0.48738, 0.80926)$.

Note that images in the left column could be obtained using various known renders, e.g., Maxwell Render [14]. Using the algorithm from [2], one can obtain the first two images in the middle column, additionally. Using the algorithm [4], one could obtain the first two images in the right column in a "draft" mode as colors would be wrong due to absence of energy calculations. The algorithm presented in this paper computes any of the nine images.

A difference between isotropic, uniaxial, and biaxial media can be clearly seen in the top row of images. In the left image (isotropic), dispersion rainbow colors are not visible (because of the camera position). In the center of image (uniaxial), birefringence is visible and the image of the cross formed by extraordinary rays is affected by dispersion. In the right image (biaxial), the both images are affected by dispersion and parts of the *transparent* crystal are colored in orange/violet hues that is a result of *dispersion of optical axes* (angle between the binormals is changed from 71.59 degree (380 nm) to 88.40 degree (780 nm)).

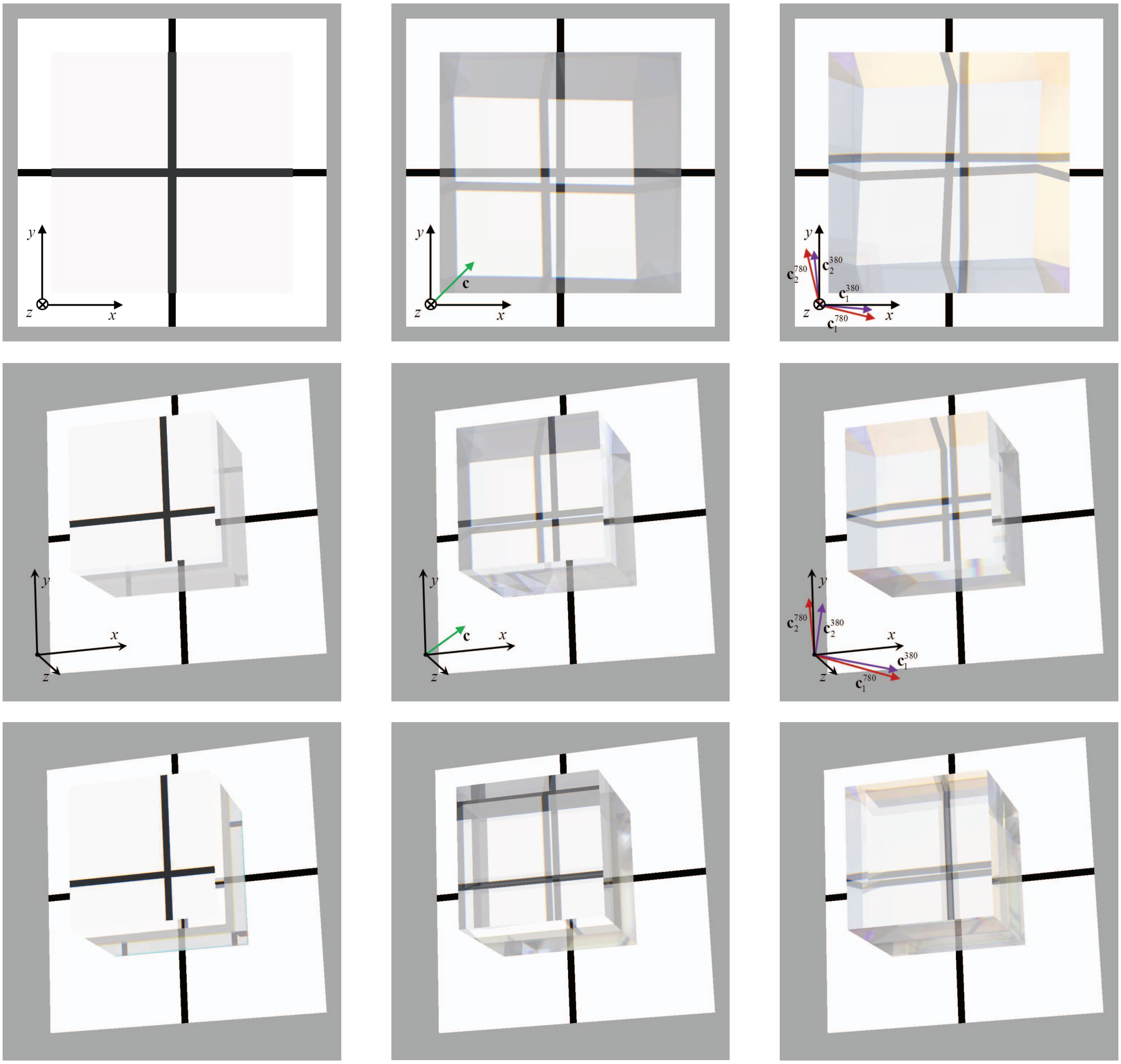

Fig. 6. Left column: isotropic; central column: uniaxial; right column: biaxial medium. Top and middle rows show monocrystals, different positions of a camera. Bottom row: crystalline aggregates.

The case of biaxial crystals is validated by rendering the effect of conical refraction. An internal conical refraction can be observed in the scene shown in Fig. 7 (left). A plate P of thickness d is made of a biaxial transparent crystal. A plate is perpendicular to one of its optical axes $\mathbf{c}_1$ (binormal), another binormal $\mathbf{c}_2$ is directed as shown in the figure. A filter F of thickness h with a cylindrical hole of a small radius r is put above the plate.

A screen S is under the plate. The construction is illuminated by unpolarized light directed parallel to the axis $\mathbf{c}_1$ and an observer sees a bright ring on the screen as in Fig. 7 (left). In practice, rays have directions close to required one but are not parallel to the axis, see Fig. 7 (right). A divergence σ of rays depends on a ratio of r and h. This results in two visible bright rings separating by a dark ring, see a real photograph [15]. In Fig. 8, there is a computed image of internal conical refraction for the modeling scene. The experimental data

1. crystal—oxammite (refractive indices: $n_1 = 1.438$, $n_2 = 1.547, n_3 = 1.595$);
2. $\mathbf{c}_1 = (0, 0, 1)$, $\mathbf{c}_2 = (0.837899, -0.304971, 0.452679)$, $\sigma = 1^\circ (r = 2.675\ \mu\text{m}, \text{h} = 613.05\ \mu\text{m}), \text{d} = 3\ \text{mm}, \text{D} = 80\ \mu\text{m}$;
3. $S : 0.8\ \text{mm} \times 0.6\ \text{mm}$ or 640×480 pixels;
4. wavelength: 550 nm.

More details about this experiment can be found in [16], [17].

9 Conclusion

In this paper, a method to calculate the outgoing rays for a given ray incident on the interface between two transparent media with different optical characteristics (isotropic,

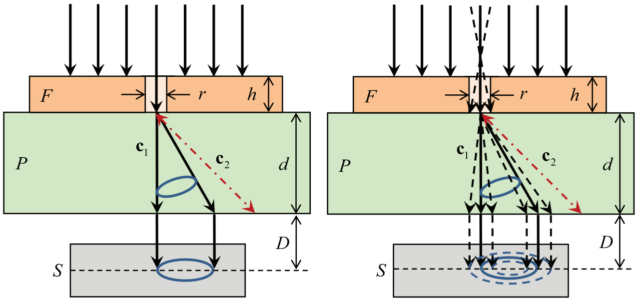

Fig. 7. Left: an ideal scene. Right: a real scene.

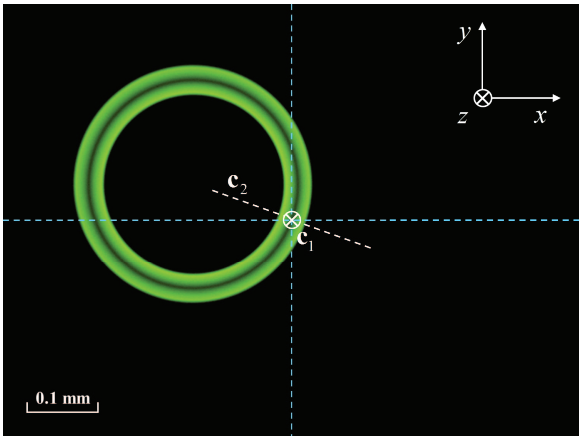

Fig. 8. A computed image of internal conical refraction.

uniaxial, or biaxial) is described. We validated the algorithm by comparing a photograph of a real uniaxial crystal with a computed image. The case of biaxial crystals is validated by testing the effect of conical refraction. In the near future, we plan to increase the accuracy of the virtual camera parameters by using camera calibration algorithms, to obtain a transparent biaxial crystal with strong birefringence, and to provide a validation process of simulation of a biaxial crystal similar to that described in the previous section for a uniaxial one. The presented algorithm can be extended to render absorbing crystals analogously to the method used in [1].

Symbol Index

To simplify reading and understanding the paper, we present a short table of most important and nonclassical symbols often used in the text with a short description for each of them.

Note that all vector variables are marked in *bold*, whereas scalars, tensors, points, and other variables are regular.

Variable	Description
$\mathbf{E}, \mathbf{e}$	vectors of electric field
$\mathbf{H}, \mathbf{h}$	vectors of magnetic field
$\mathbf{p}$	ray (energy) propagation vector
$\mathbf{m}$	phase (wave-front) propagation vector
$\mathbf{n}$	unit phase propagation vector
n, n_γ	phase and main refractive indices
$\mathbf{c}$	optical axis in uniaxial medium
$\mathbf{c}_1, \mathbf{c}_2$	binormals in biaxial medium
$\varepsilon, \varepsilon_\gamma$	permittivity tensor and principal permittivities
λ	wavelength in vacuum
$\mathbf{x}, \mathbf{y}, \mathbf{z}$	ray coordinate system
ω	wave circular frequency
ϕ	wave phase
Q	point of incident
Σ	tangent plane to boundary at point Q
Π	plane of incidence formed by $\mathbf{q}$ and $\mathbf{m}$
$\mathbf{q}$	unit normal to plane Σ
$\mathbf{u}$	unit normal to plane Π
$\mathbf{v}$	unit vector in $\Sigma \cap \Pi$
$\mathbf{g}$	projection of vector $\mathbf{m}$ on plane Σ
$\mathbf{r}$	radius-vector with origin at point Q

Subscript	Description
0	incident wave
r, t	reflected and transmitted waves
i	wave in isotropic medium
o, e	ordinary, extraodinary waves (uniaxial)
$+, -$	plus and minus waves (biaxial)

Operator	Description
$\mathbf{ab}$	dot product of vectors $\mathbf{a}$ and $\mathbf{b}$
$[\mathbf{ab}]$	vector product of vectors $\mathbf{a}$ and $\mathbf{b}$
$\mathbf{a} \cdot \mathbf{b}$	dyad of vectors $\mathbf{a}$ and $\mathbf{b}$
$\bar{\alpha}$	adjoint matrix to matrix α
α_t	trace of matrix α
$\mathbf{a}^\times$	dual tensor to vector $\mathbf{a}$
$\alpha\mathbf{b}$	product of matrix α and vector $\mathbf{b}$
$\lvert\alpha\rvert$	determinant of matrix α

Acknowledgments

This work was supported in part by the grants Nos. 12-07-00386 and 12-07-00391 of Russian Foundation for Basic Research. The authors would like to thank a crystallographer Dr. Sergey Z. Smirnov for valuable advices, Yuri A. Dankin who created faceted crystals of calcite, and to the first user of the algorithm Prof. Alexander M. Matsokin who found important typos in the paper.

References

[1] S. Guy and C. Soler, "Graphics Gems Revisited," *ACM Trans. Graphics,* vol. 23, no. 3, pp. 231-238, Aug. 2004.

[2] A. Weidlich and A. Wilkie, "Realistic Rendering of Birefringency in Uniaxial Crystals," *ACM Trans. Graphics,* vol. 27, no. 1, pp. 6:1-6:12, 2008.

[3] V.A. Debelov and D.S. Kozlov, "A Local Model of Light Interaction with Isotropic and Uniaxial Transparent Media," *Vestnik of Novosibirsk State Univ., Series: Information Technologies,* vol. 10, no. 1, pp. 5-23, 2012.

[4] P. Latorre, F. Seron, and D. Gutierrez, "Birefringence: Calculation of Refracted Ray Paths in Biaxial Crystals," *Visual Computer,* vol. 28, pp. 341-356, 2012.

[5] Y. Wang, P. Shi, H. Xin, and L. Wu, "Complex Ray Tracing in Biaxial Anisotropic Absorbing Media," *J. Optics A: Pure and Applied Optics,* vol. 10, no. 7, p. 075009, 2008.

[6] S.C. McClain, L.W. Hillman, and R.A. Chipman, "Polarization Ray Tracing in Anisotropic Optically Active Media. 2. Theory and Physics," *J. Optical Soc. Am.,* vol. 10, no. 11, pp. 2383-2393, Nov. 1993.

[7] F.I. Fedorov and V.V. Filippov, *Reflection and Refraction of Light by Transparent Crystals,* Minsk: "Nauka i Tekhnika," 1976.

[8] M. Born and E. Wolf, *Principles of Optics: Electromagnetic Theory of Propagation, Interference and Diffraction of Light.* Cambridge Univ. Press, 1980.

[9] D.C. Tannenbaum, P. Tannenbaum, and M.J. Wozny, "Polarization and Birefringency Considerations in Rendering," *Proc. ACM SIGGRAPH,* A. Glassner, ed., pp. 221-222, 1994.

[10] C.M. Goral, K.E. Torrance, D.P. Greenberg, and B. Battaile, "Modeling the Interaction of Light between Diffuse Surfaces," *Proc. 11th Ann. Conf. Computer Graphics and Interactive Techniques,* pp. 213-222, 1984.

[11] G.W. Meyer, H.E. Rushmeier, M.F. Cohen, D.P. Greenberg, and K.E. Torrance, "An Experimental Evaluation of Computer Graphics Imagery," *ACM Trans. Graphics,* vol. 5, pp. 30-50, Jan. 1986.

[12] T. Whitted, "An Improved Illumination Model for Shaded Display," *Comm. ACM,* vol. 23, no. 6, pp. 343-349, 1980.
[13] A.S. Glassner, "How to Derive a Spectrum from an RGB Triplet," *IEEE Computer Graphics Applications,* vol. 9, no. 4, pp. 95-99, July 1989.
[14] Maxwell render, http://www.maxwellrender.com, 2013.
[15] Y.P. Mikhaylichenko, *Large Scale Experiments on Conical Refraction,* http://www.demophys.tsu.ru/Original/Hamilton/Hamilton.html, Dec. 2004.
[16] V.A. Debelov and D.S. Kozlov, "Verification of Algorithms of Photorealistic Rendering of Crystals," *Proc. 20th Int'l Conf. Computer Graphics and Vision Graphicon-2010,* http://www.graphicon.ru/proceedings/2010/conference/RU/Se5/04.pdf, pp. 238-245, Sept. 2010.
[17] V.A. Debelov and D.S. Kozlov, "Rendering of Translucent Objects, Verification and Validation of Algorithms," *Proc. 20th Int'l Conf. Central Europe on Computer Graphics, Visualization and Computer Vision,* http://wscg.zcu.cz/wscg2012/CD-ROM/WSCG-2012-CD-ROM.zip, June 2012.

Victor A. Debelov received the graduation degree from Novosibirsk State Technical University in 1975 and the PhD degree in computer science and engineering from the Institute of Computational Mathematics and Mathematical Geophysics (ICM&MG) (former Computing Center) in 1979. He is with the Laboratory of Numerical Analysis and Computer Graphics, ICM&MG, Siberian Branch of Russian Academy of Sciences. He holds a position of leading researcher. Also, he is a part-time professor in the Department of Information Technologies at Novosibirsk State University. His current interests concern photorealistic rendering of crystals, computer models of crystal growth, scientific visualization in crystallography.

Dmitry S. Kozlov received the master's degree in computer science from Novosibirsk State University in 2008. He is working toward the PhD degree in the Laboratory of Numerical Analysis and Computer Graphics at the Institute of Computational Mathematics and Mathematical Geophysics, Siberian Branch of Russian Academy of Science. He is currently a software developer for DataEast LLC in Novosibirsk from 2007 to present. His research interests lie in the area of photorealistic rendering of crystals and scientific visualization in crystallography.